Topical Application of Human Wharton's Jelly Mesenchymal Stem Cells Accelerates Mouse Sciatic Nerve Recovery and is Associated with Upregulated Neurotrophic Factor Expression

Aline Yen Ling Wang[1] , Charles Yuen Yung Loh[2], Hsin-Hsin Shen[3],
Sing-Ying Hsieh[3], Ing-Kae Wang[3], Sheng-Hao Chuang[1],
and Fu-Chan Wei[1,4,5]

Abstract

Peripheral nerve regeneration following injury is often slow and impaired, which results in weakened and denervated muscle with subsequent atrophy. Human Wharton's jelly mesenchymal stem cells (hWJ-MSC) have potential regenerative properties which, however, remain unknown in mouse nerve recovery. This study investigated the effect of the topical application of hWJ-MSC onto repairing transected sciatic nerves in a mouse model. Human adipocyte-derived stem cells (hADSC) were used as a positive control. The sciatic nerve of BALB/c mice was transected at a fixed point and repaired under the microscope using 10-0 sutures. hWJ-MSC and hADSC were applied to the site of repair and mice were followed up for 1 year. The hWJ-MSC group had significantly better functional recovery of five-toe spread and gait angles compared with the negative control and hADSC groups. hWJ-MSC improved sciatic nerve regeneration in a dose-dependent fashion. The hWJ-MSC group had a better quality of regenerated nerve with an increased number of myelinated axons throughout. hWJ-MSC appear to be safe in mice after 1 year of follow-up. hWJ-MSC also expressed higher levels of neurotrophic factor-3, brain-derived neurotrophic factor, and glial-derived neurotrophic factor than hADSC. hWJ-MSC may promote better nerve recovery than hADSC because of this upregulation of neurotrophic factors.

Keywords

Introduction

Injured peripheral nerves generally have difficulty in regenerating and patients are often left with long-lasting neural deficits[1–6]. Peripheral nerve injuries commonly occur as part of trauma or iatrogenically during excision or removal of an adjacent lesion. With the recent interest in vascularized composite allotransplantation, that is, transplantation of a whole limb, the face, or the abdominal wall[7–9] to restore function and appearance, the recovery of repairing peripheral nerves becomes crucial for restoration of good graft function[10–14]. Of the various types of nerve injury, complete transection has the worst outcome for regeneration. When reinnervation of the transected peripheral nerve is delayed or poor, the motor endplates of the target muscles degenerate, resulting

[1] Center for Vascularized Composite Allotransplantation, Chang Gung Memorial Hospital, Taoyuan, Taiwan
[2] St Andrew's Center for Burns and Plastic Surgery, Chelmsford, UK
[3] Biomedical Technology and Device Research Laboratories, Industrial Technology Research Institute, Hsinchu, Taiwan
[4] Department of Plastic Surgery, Chang Gung Memorial Hospital, Taoyuan, Taiwan
[5] College of Medicine, Chang Gung University, Taoyuan, Taiwan

Corresponding Author:
Aline Yen Ling Wang, Center for Vascularized Composite Allotransplantation, Chang Gung Memorial Hospital, 5, Fu-Hsing Street, Gueishan, Taoyuan 333, Taiwan.
Email: aline2355@yahoo.com.tw

in muscle atrophy that can affect the function of the limb[15–19]. Early and effective repair of the injured peripheral nerves allows optimal regeneration and hence is crucial to preserving limb function.

Recent interest in the mesenchymal stem cells (MSC) and their multipotent potential has led to an expansion in research involving regeneration of tissue[20], in particular, the umbilical cord and Wharton's jelly-derived MSC[21,22]. Wharton's jelly of the umbilical cord contains mucoid connective tissue and fibroblast-like cells, among which MSC can be identified and isolated. It has been shown that these MSC can be differentiated into cells of various lineages[23]. Human Wharton's jelly-derived MSC (hWJ-MSC) have also demonstrated low immunogenicity[24,25], making them ideal for use in cell therapeutics. Several studies have demonstrated the efficacy of human adipocyte-derived stem cells (hADSC) in improving peripheral nerve regeneration. Therefore, we used hADSC as a positive control in this study to compare with hWJ-MSC[26–29].

This study examined the direct effects of hWJ-MSC on nerve regeneration in a mouse model of simple transection mimicking that commonly encountered in clinical practice. Provided hWJ-MSC can be demonstrated in animal models to augment directly the recovery of peripheral nerves, their use in humans would be ideal. To our knowledge, this study is the first to examine the possibility of using hWJ-MSC to enhance peripheral nerve regeneration in a mouse model of complete transection and repair of the sciatic nerve.

Materials and Methods

Mice

All procedures carried out in the study were fully compliant with the recommendations stipulated by the Guide for the Care and Use of Laboratory Animals (Chang Gung Memorial Hospital Animal Research Guidelines). Animal protocols were approved by the Committee on the Ethics of Animal Experiments of the Chang Gung Memorial Hospital (CGMH) in Taiwan and Institutional Animal Care and Use Committees (IACUC) of CGMH in Taiwan under permit numbers IACUC 2016011903, IACUC 2016031109, IACUC 2017121001, IACUC 2018080701. The 6–8-week-old BALB/c mice used in our study were purchased from the National Laboratory Animal Center, Taiwan. The mice were cared for in an enriched environment with an abundance of nesting material. The mice were monitored daily, and any mice showing a drop in weight or displaying the inability to seek food or other signs of illness were euthanized.

Culture of hWJ-MSC and hADSC

Dr. Hsin-Hsin Shen from the Industrial Technology Research Institute of Taiwan (ITRI) provided hWJ-MSC and hADSC that had been purchased from the Food Industry Research Development Institute and ScienCell Research Laboratories, respectively. The stem cells were maintained in a humidified chamber at 37°C and 5% CO_2 in SF1 hMSC medium (Unimed Healthcare Inc., Taipei, Taiwan) and maintained until 80% confluent. For cell passage, cells were washed with phosphate-buffered saline (PBS) then treated with trypsin (TrypLE^{TM} Select; Thermo Fisher Scientific, Waltham, MA, USA). Trypsin was inactivated by addition of SF1 hMSC medium and cells were centrifuged at 1200 rpm for 5 min. Cell viability was evaluated using the trypan blue exclusion method.

Mouse Sciatic Nerve Transection Model

The sciatic nerves of mice were surgically transected as described previously[30,31]. Mice were anesthetized with inhaled isoflurane and the entire hindlimb of the mouse was shaved and cleaned with 75% methyl ethanol. A longitudinal incision was then made in the skin directly over the course of the sciatic nerve. The plane between the gluteal muscles was then exposed by blunt dissection. The sciatic nerve was identified and divided 1 cm proximal to the trifurcation of the nerve. Epineural repair of the nerve was performed under an operative microscope with 25× magnification using four evenly spaced 10-0 nylon sutures.

Topical Administration of MSC and Buffer Control

After division and coaptation of the sciatic nerve, a suspension of hWJ-MSC, hADSC, or buffer negative control was added to the space created in the musculature. The same volume (50 μl) and number of cells (5×10^5) were added in each mouse, as shown in Figs 1 and 2. The negative control group had PBS added alone without any cells. The skin was then sutured closed and restored to its appropriate anatomical state. There were no transection of nerves and administration of cells in the normal control group.

Methods to Assess Functional Recovery

Five-toe spread analysis. The recovery of the five-toe reflex of mice after nerve transection is a sensitive indicator of intrinsic muscle recovery[32,33]. Five-toe spread measurements were taken and recorded every week. The distance between the first and last toe was measured using calibrated calipers. Four replicate recordings were made for each mouse and the average score was used. Each five-toe spread distance measurement was expressed as a percentage of the pre-transection distance to monitor recovery. The distance was plotted against time and the greater the toe spread distance, the better the nerve recovery.

Video gait angle analysis. The regeneration of peripheral nerves affects the innervation and maintenance of muscle bulk that permits normal gait. In particular, the sciatic nerve innervates a large volume of muscle that controls movement at the ankle level. Therefore, the ankle movements of the mice during walking are affected during recovery. At various gait
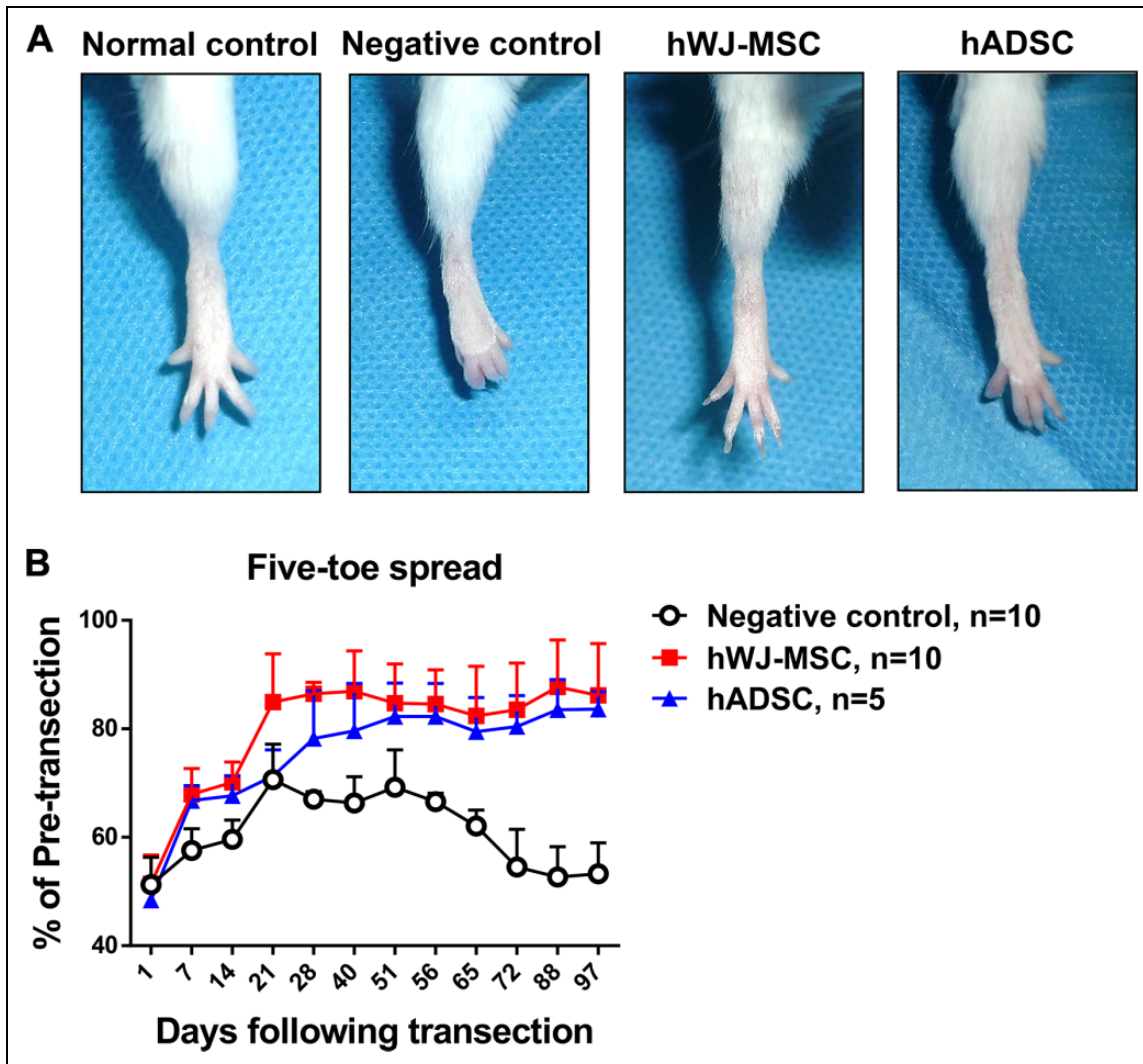
Figure 1. Five-toe spread measurement and analysis over time. (A) Serial photographs of five-toe spread at postoperative day 60 in normal control, negative control, human Wharton's jelly mesenchymal stem cells (hWJ-MSC), and human adipocyte-derived stem cells (hADSC). After division and coaptation of the sciatic nerve, a suspension of hWJ-MSC, hADSC, or PBS negative control was added to the space created in the musculature. The same number of stem cells (5×10^5) was added in both hWJ-MSC and hADSC groups at postoperative day (POD) 0. There were no transection of nerves and administration of cells in the normal control group. (B) Progressive chart of the percentage of the pre-transection five-toe spread distance measured over time following division of the sciatic nerve in negative control, hWJ-MSC, and hADSC groups. The mean $\pm$ SD of the negative control, hWJ-MSC, and hADSC groups were 67.0 $\pm$ 1.4%, 86.5 $\pm$ 2.1%, and 78.2 $\pm$ 8.7%, respectively, at POD 28. The mean $\pm$ SD of the negative control, hWJ-MSC, and hADSC groups were 62.1 $\pm$ 2.9%, 82.4 $\pm$ 9.2%, and 79.5 $\pm$ 6.3%, respectively, at POD 65. The differences between mean $\pm$ SD of the hWJ-MSC and hADSC groups and the negative control were significant (*p* value < 0.0001, one-way ANOVA; negative control vs. hWJ-MSC, $p = 0.0001$; negative control vs. hADSC, $p = 0.0017$; hWJ-MSC vs. hADSC, $p = 0.0033$; Tukey's test). The average five-toe spread in the normal mouse group was 9.911 $\pm$ 0.04832 mm.

phases, the ankle angles created are indicative of the isometric force generated to lift the mouse's body weight off the floor[34]. There are four main stages of the mouse gait cycle: foot on ground, midstance, toe-off phase, and the mid-swing phase. The angles measured during the toe-off phase have been shown to correlate with muscle strength and sciatic nerve recovery.

A walking track apparatus was used to guide the mice and a 60 Hz digital image camera was used to record the gait motion. The recording was then repeated for four attempts at walking; the ankle angles were measured for each and the average calculated.

Stereographic Analysis of Cross-Sectional Nerve Recovery

Cross-sectional staining of axons with toluidine blue and examination under a microscope allows for accurate analysis of the degree of axonal regrowth. The ratio of axon diameter to nerve fiber diameter (g-ratio) is an indicator of the quality
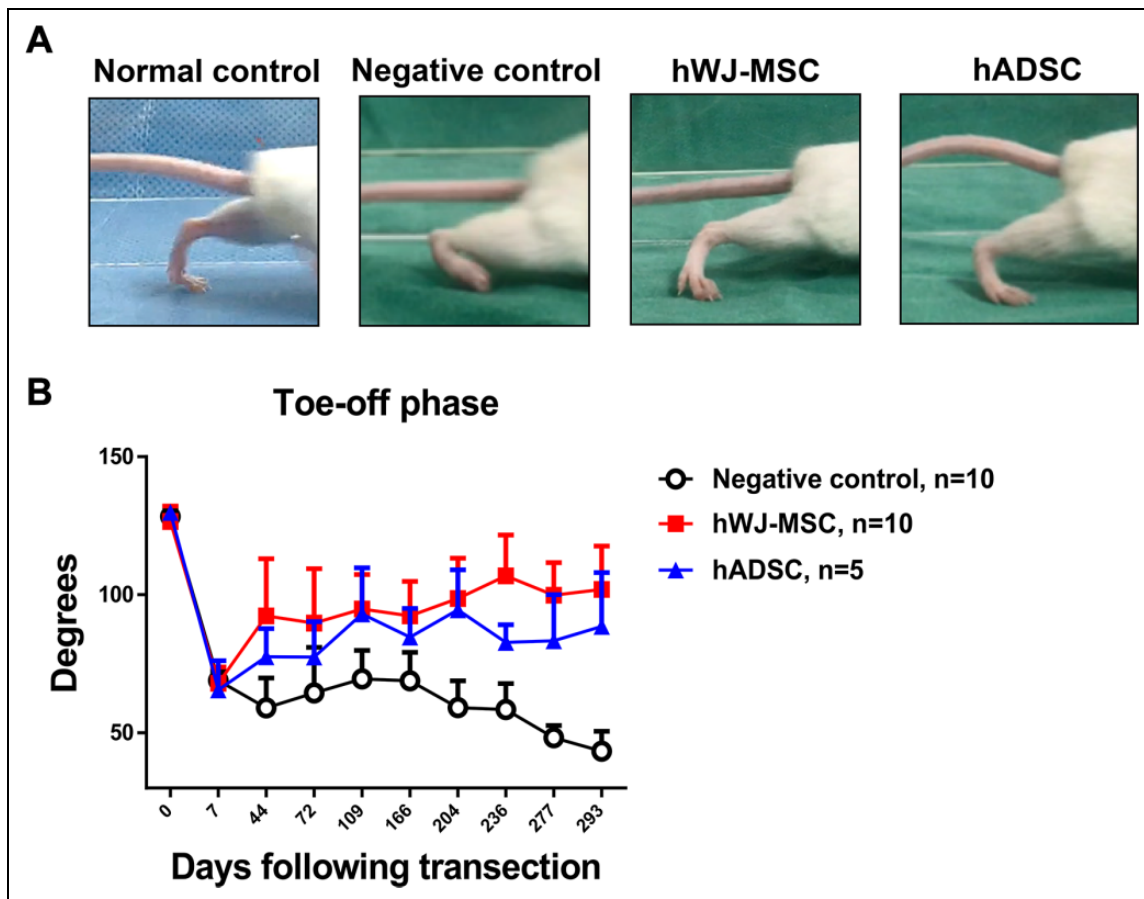
Figure 2. Video gait analysis and measurement of gait angles. (A) Photographs of mouse gait angles at the toe-off phase of the gait cycle at 236 days postoperatively in normal control, negative control, hWJ-MSC, and hADSC. The same number of stem cells (5×10^5) was added in both hWJ-MSC and hADSC groups at postoperative day 0. (B) Angles were measured in the negative control, hWJ-MSC, and hADSC groups for up to 293 days following transection surgery. The mean $\pm$ SD of the negative control, hWJ-MSC, and hADSC groups were $68.9 \pm 3.4°$, $68.0 \pm 5.8°$, and $65.5 \pm 10.6°$, respectively, at POD 7. The mean $\pm$ SD of the negative control, hWJ-MSC, and hADSC groups were $59.1 \pm 10.8°$, $92.4 \pm 20.6°$, and $77.5 \pm 10.3°$, respectively, at POD 44. The mean $\pm$ SD of the negative control, hWJ-MSC, and hADSC groups were $58.5 \pm 9.3°$, $106.8 \pm 14.9°$, and $82.8 \pm 6.4°$, respectively, at POD 236. Comparison of mean $\pm$ SD of the negative control with hWJ-MSC and hADSC groups showed a significant difference ($p = 0.0008$, one-way ANOVA; negative control vs. hWJ-MSC, $p = 0.0030$; negative control vs. hADSC, $p = 0.0048$; hWJ-MSC vs. hADSC, $p = 0.0149$; Tukey's test). The average angle of the normal mouse group was $128.0° \pm 0.8376°$.

of regrowth of regenerated axons and their ability to conduct an electric signal. The operated sciatic nerve was evaluated at a fixed distance of 7 mm distal to the point of initial repair. This segment of nerve was then further subdivided at the halfway mark (3.5 mm). The nerves were then stained with toluidine blue and divided into ultrathin 60-nm sections, poststained with lead citrate and uranyl acetate and examined under a light microscope[35,36]. Stereographic analysis of the sciatic nerve sections was then performed to document the density of axons, and the g-ratio.

Real-Time Polymerase Chain Reaction (qPCR)

hWJ-MSC and hADSC were cultured and mRNA was extracted and converted to complementary DNA (cDNA). The mRNA expression was analyzed with TaqMan gene expression assays (Thermo Fisher Scientific). To examine for neurotrophic growth factors, brain-derived neurotrophic growth factor (BDNF: Hs02718934_s1), glial-derived neurotrophic factor (GDNF: Hs01931883_s1), neurotrophic growth factor (NGF: Hs00171458_m1), and neurotrophic factor 3 (NT-3: Hs00267375_s1) mRNA levels were quantified using qPCR. The neurotrophic factor expression in this study was normalized to that of glyceraldehyde 3-phosphate dehydrogenase (GAPDH: Hs02786624_g1).

Statistical Analysis

Data were expressed as mean $\pm$ SD and the significance of differences between groups was evaluated using the two-tailed Student's *t*-test. The differences between mouse groups for five-toe spread and gait analysis were calculated

by one-way analysis of variance (ANOVA) using SPSS 17.0 (SPSS Inc., Chicago, IL, USA) with post hoc analysis by Tukey's multiple comparisons test. A p value of <0.05 was considered significant.

Results

hWJ-MSC Accelerate Functional Recovery of the Five-Toe Spread Reflex

To evaluate the potential effect of hWJ-MSC on mouse peripheral nerve recovery, we analyzed the five-toe spread distance, a sensitive indicator of intrinsic muscle recovery[32,33]. At postoperative day (POD) 60, the hWJ-MSC group and the hADSC groups showed full abduction of the toes, almost similar to the normal five-toe spread (Fig. 1A). However, the feet of the negative control group remained in a clawed position secondary to contracture of the small muscles of the foot.

The hindlimb recovery curves of both MSC groups were significantly improved compared with that of the negative control (Fig. 1B). The hWJ-MSC group exhibited significantly better functional recovery than the positive control hADSC group as assessed by five-toe spread analysis. The hWJ-MSC group reached $86.5 \pm 2.1\%$ of the preoperative distance within 28 days, compared with the negative control and hADSC groups that reached $67.0 \pm 1.4\%$ and $78.2 \pm 8.7\%$ of the preoperative distance, respectively. The negative control, hWJ-MSC, and hADSC groups showed $62.1 \pm 2.9\%$, $82.4 \pm 9.2\%$, and $79.5 \pm 6.3\%$, respectively, at POD 65. The percentages (mean $\pm$ SD) of the pre-transection five-toe spread distance measured over time between the three groups are shown in Supplementary Table 1. The hWJ-MSC group maintained their five-toe spread distance because of quicker reinnervation compared with the negative control. Subsequent contracture of the small muscles of the foot was the main cause for the reduction in the spread distance.

hWJ-MSC Restore Normal Gait Stance and Movement

The stage 3 toe-off gait phase has been shown to correlate most strongly with sciatic nerve recovery[34]. The mouse requires adequate muscle recovery to generate enough strength to lift off. Measurement of the ankle angles can determine the degree of muscle and nerve recovery: the larger the angle, the better the muscle recovery. Ankle angles eventually reduce in amplitude because of contracture formation. At POD 236, the photograph in Fig. 2A of the normal group shows the normal large ankle angle that is only present with a fully intact sciatic nerve. The ankle angle seen in the negative control group was the smallest because of the lack of full sciatic nerve recovery. The hWJ-MSC and hADSC groups both demonstrated larger ankle angles than the negative control group, which were close to the ankle angles seen in normal mice.

At POD 7, there was a sharp initial decrease (negative control: $68.9 \pm 3.4°$, hWJ-MSC: $68.0 \pm 5.8°$, and hADSC: $65.5 \pm 10.6°$) in the angles measured because of the loss of innervation of the flexor muscles, indicating that plantar flexion is not possible after nerve division. The negative control, hWJ-MSC, and hADSC groups showed $58.5 \pm 9.3°$, $106.8 \pm 14.9°$, and $82.8 \pm 6.4°$, respectively, at POD 236. The gait angles (mean $\pm$ SD) measured over time between negative control, hWJ-MSC, and hADSC groups are shown in Supplementary Table 2. Throughout the follow-up period, the negative control group showed persistently low angles that did not generate enough muscle force to lift the mouse's body weight. The hWJ-MSC group exhibited significantly better functional recovery than the negative control and hADSC groups as assessed by gait angle analysis. The hWJ-MSC group displayed a gradual but steady rise in the angles measured during the toe-off phase, which was indicative of muscle reinnervation and preservation of muscle bulk and strength (Fig. 2B).

The results from this measurement demonstrated that the hWJ-MSC group showed significant acceleration of the recovery and maintenance of the muscles responsible for gait, which was not seen in the negative control group within the same time period.

Higher Doses of hWJ-MSC Promote an Enhanced Level of Peripheral Nerve Recovery

Because the five-toe spread and gait stance analyses indicated that the hWJ-MSC group exhibited better functional recovery than the hADSC group, we next evaluated whether the efficacy of peripheral nerve recovery was dependent on the dose of hWJ-MSC. Three different groups of mice had varying numbers of hWJ-MSC added to the site of sciatic nerve repair. The three groups received low, medium, and high numbers of hWJ-MSC (1×10^5, 5×10^5, and 10×10^5, respectively). The five-toe spread distance in each group was then measured over time to determine whether a higher dose of cells increased the rate of nerve regeneration. At POD 21, the negative control, hWJ-MSC-L, hWJ-MSC-M, and hWJ-MSC-H groups showed $75.6 \pm 6.6\%$, $81.1 \pm 14.7\%$, $86.0 \pm 9.7\%$, and $91.9 \pm 4.8\%$, respectively. The negative control, hWJ-MSC-L, hWJ-MSC-M, and hWJ-MSC-H groups showed $59.0 \pm 10.8\%$, $83.1 \pm 14.3\%$, $84.1 \pm 9.9\%$, and $91.8 \pm 6.3\%$, respectively, at POD 76. The percentages (mean $\pm$ SD) of the pre-transection five-toe spread distance measured over time between the four groups are shown in Supplementary Table 3. All three doses produced a significantly quicker restoration of the five-toe spread distance than that seen in the negative control. The group that received the highest dose of hWJ-MSC showed a significantly increased five-toe spread distance compared with the medium- and low-dose groups (Fig. 3).
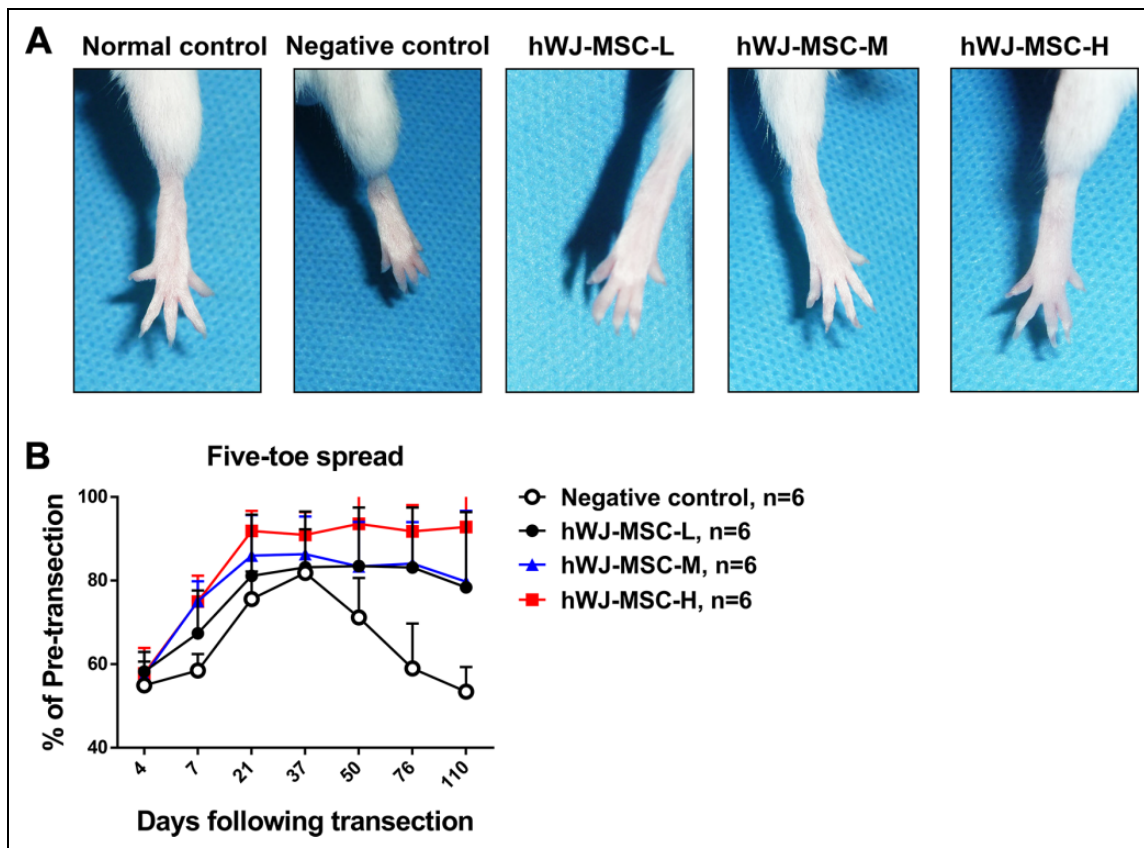
Figure 3. Five-toe spread measurements in mice receiving various doses of hWJ-MSC. (A) Serial photographs of five-toe spread at postoperative day 76 in normal control, negative control, hWJ-MSC-L (1×10^5 cells), hWJ-MSC-M (5×10^5 cells) and hWJ-MSC-H (10×10^5 cells) groups (where suffixes –L, -M, and –H mean low, medium, and high numbers of hWJ-MSC, respectively). (B) Five-toe spread measurements for hWJ-MSC-L, hWJ-MSC-M, and hWJ-MSC-H groups. The mean $\pm$ SD of the negative control, hWJ-MSC-L, hWJ-MSC-M, and hWJ-MSC-H groups were $75.6 \pm 6.6\%$, $81.1 \pm 14.7\%$, $86.0 \pm 9.7\%$, and $91.9 \pm 4.8\%$, respectively, at POD 21. The mean $\pm$ SD of the negative control, hWJ-MSC-L, hWJ-MSC-M, and hWJ-MSC-H groups were $71.2 \pm 9.4\%$, $83.5 \pm 14.0\%$, $83.4 \pm 10.7\%$, and $93.6 \pm 8.0\%$, respectively, at POD 50. The mean $\pm$ SD of the negative control, hWJ-MSC-L, hWJ-MSC-M, and hWJ-MSC-H groups were $59.0 \pm 10.8\%$, $83.1 \pm 14.3\%$, $84.1 \pm 9.9\%$, and $91.8 \pm 6.3\%$, respectively, at POD 76. The statistical comparison of mean $\pm$ SD of the negative control group with the other groups showed a significant difference ($p = 0.0047$, one-way ANOVA; negative control vs. hWJ-MSC-M, $p = 0.0291$; negative control vs. hWJ-MSC-H, $p = 0.0242$; hWJ-MSC-L vs. hWJ-MSC-H, $p = 0.011$; Tukey's test). The average five-toe spread in the normal mouse group was 9.911 ± 0.04832 mm.

hWJ-MSC Improve the Quality of Axonal Regeneration

Quantitative stereographical histological analysis of the quality of peripheral nerve regeneration was performed to confirm the above findings. Direct examination of sciatic nerve axonal regeneration in each group of mice was performed 1 year postoperatively using toluidine blue staining. The histological structures of axons and nerve fibers are shown in Fig. 4A. The hWJ-MSC and hADSC groups showed an overall greater density of axons compared with the negative control. In the proximal section of the regenerated nerve, axons were generally larger in size compared with the smaller axons in the distal end, which represent newly regenerated axons. The distal-section axons were greater in number and more evenly distributed throughout the cross-section of the nerve in both hWJ-MSC and hADSC groups than in the negative control group (Figs 4A–4E).

In the section of the regenerated sciatic nerve proximal to the transection, where ingrowth of axons is expected to be normal with intact architecture and substance of the peripheral nerve, the total axon count and total axonal area were similar in hWJ-MSC, hADSC, negative and normal control groups after 1 year (Figs 4B and 4C). However, there were a significantly greater number of axons and a greater total axonal surface area in the distal end of the sciatic nerve of the hWJ-MSC, hADSC, and normal group compared with that in the distal end of the negative control group (Figs 4D and 4E).

The g-ratio evaluates the amount of myelination in relation to axon diameter, which in turn, can be used to assess the degree of nerve regeneration. It provides a method of evaluating nerve conduction velocity and fiber morphology during peripheral nerve regeneration. The g-ratio is somewhat
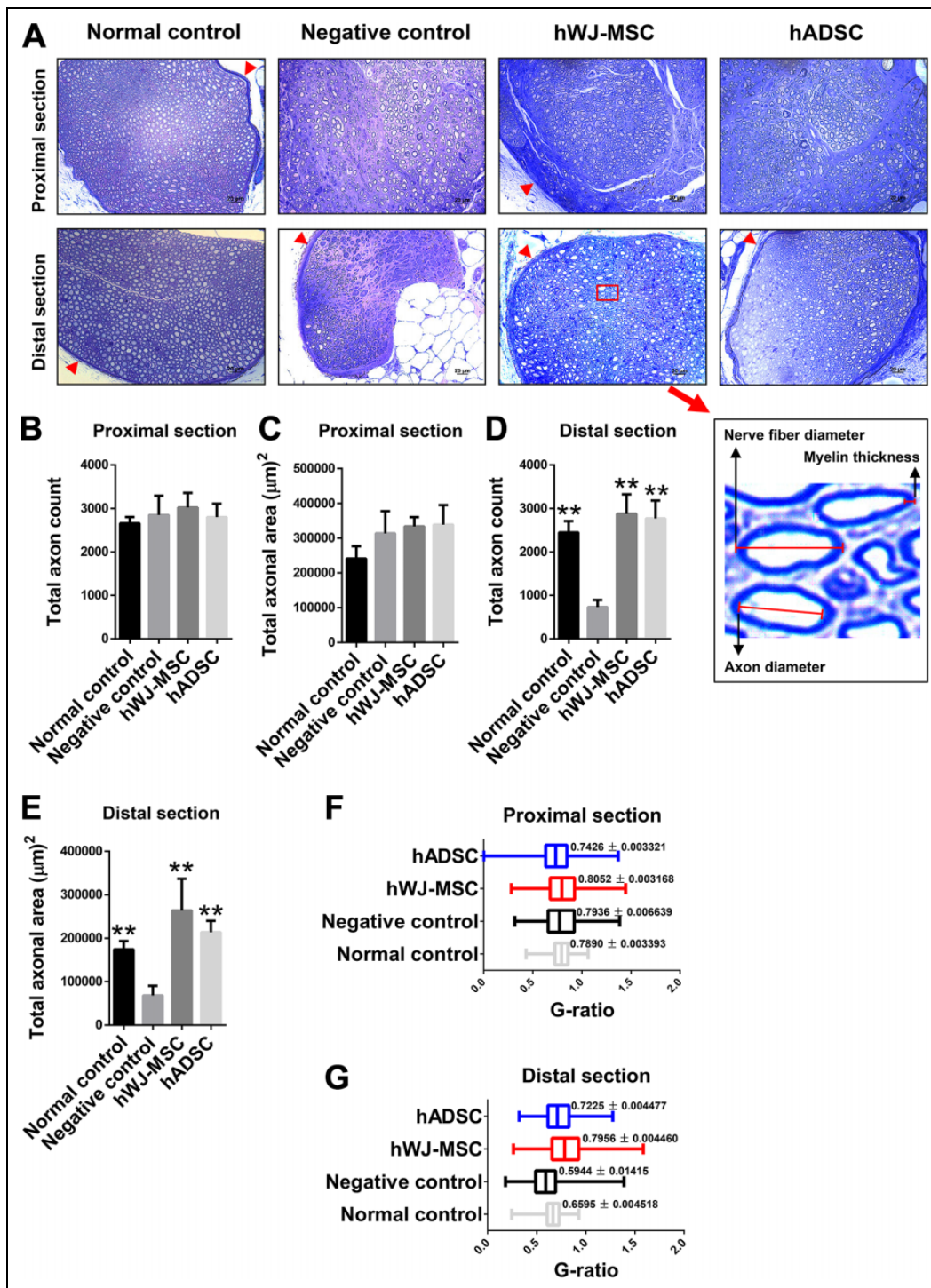
Figure 4. Stereographic analysis of sciatic nerves from hWJ-MSC, hADSC, negative control, and normal control groups. (A) Microscopic examination of cross-sectional, toluidine blue-stained proximal and distal sciatic nerve ends from all four groups at postoperative day 360. The same number of stem cells (5×10^5) was added in both hWJ-MSC and hADSC groups at postoperative day 0. The red arrow represents the perineurium. The photographs below show the histological structures of nerve fiber, axon, and myelin. Proximal-end total axon count (B) and total axonal area (C). The mean $\pm$ SD of the normal control, negative control, hWJ-MSC, and hADSC groups were 2660 ± 142.7, 2848 ± 443.4, 3021 ± 336.9, and 2798 ± 311.2, respectively, for the proximal-end total axon counts. The mean $\pm$ SD of the normal control, negative control, hWJ-MSC, and hADSC groups were 241337 ± 35452, 313594 ± 63821, 333740 ± 26457, and 338537 ± 56189, respectively, for the proximal-end total axonal area $(\mu m)^2$. Distal-end total axon count (D) and total axonal area (E). The mean $\pm$ SD of the normal control, negative control, hWJ-MSC, and hADSC groups were 2448 ± 259.6, 729.9 ± 163.8, 2875 ± 451.5, and 2769 ± 413.3, respectively, for the distal-end total axon counts. The mean $\pm$ SD of the normal control, negative control, hWJ-MSC, and hADSC groups were 174369 ± 19047, 68113 ± 22278, 263644 ± 73357, and 213500 ± 26312, respectively, for the distal-end total axonal area $(\mu m)^2$. (F, G) The g-ratio comparing the proximal (F) and distal (G) sections of regenerated sciatic nerves in the four groups. The statistical comparison of mean $\pm$ SD of the negative control group with the other groups showed a significant difference ($p < 0.005$, Student's *t*-test).

higher (i.e., relatively thinner myelin) for small myelinated axons but generally varies between 0.5 and 0.8 for all fibers[37–42]. In the proximal area of the sciatic nerve, the g-ratio across all groups was 0.74–0.80, indicating similar regeneration. In the distal area, hADSC (0.72 ± 0.01) and hWJ-MSC (0.79 ± 0.01) groups both had higher g-ratios than the negative control (0.59 ± 0.01) (Figs 4F and 4G).

hWJ-MSC Appear to have no Adverse Effects in Mice

The mice in each group were followed up for 1 year to examine the systemic and long-term effects of hWJ-MSC. hWJ-MSC and hADSC groups maintained $78.1 \pm 13.1\%$ and $69.3 \pm 8.1\%$, respectively, of the pre-transection five-toe spread distance, which was significantly higher than the $46.4 \pm 5.6\%$ seen in the negative control group at post-operative day 360. The percentages (mean $\pm$ SD) of the pre-transection five-toe spread distance measured over 1 year between the three groups are shown in Supplementary Table 4. Long-term observation indicated that hWJ-MSC resulted in significantly better hindlimb recovery of five-toe spread than hADSC (Fig. 5A). All mice displayed normal behavior and were feeding as normal. One year after surgery, mice were sacrificed and the area of cell application was examined macroscopically (Fig. 5B). The photographs show that anatomical structures were maintained with no abnormalities or growths detected in hWJ-MSC, hADSC, negative, and normal control groups. Hematoxylin and eosin staining of the major organs of heart, liver, intestine, kidney, and spleen was also performed to look for any microscopic abnormalities or disruption to regular cellular architecture. Only a small number of infiltrating inflammatory cells were observed in some organs. There was no evidence of any invasive tumors or abnormal cellular growths in all groups (Fig. 5C).

hWJ-MSC Accelerate and Improve Peripheral Nerve Regeneration and may be Associated with Increased Levels of NT-3, BDNF and GDNF

Neurotrophic factors such as NT-3, BDNF, NGF, and GDNF are involved in the repair of peripheral nerves[30]. These molecules exert their effects on nearby structures and peripheral nerves through a paracrine route. To determine whether there were differences in neurotrophic factor expression that could be responsible for the above findings, we analyzed the expression of mRNA for NT-3, BDNF, NGF, and GDNF in hWJ-MSC and hADSC. hWJ-MSC expressed higher levels of NT-3, BDNF, and GDNF mRNA compared with hADSC (Fig. 6).

Discussion

This study showed that the application of hWJ-MSC to transected and repaired sciatic nerves of mice can have profound effects on improving and maintaining well-regenerated peripheral nerve substance. Functionally, preservation of the five-toe spread distance was seen in the hWJ-MSC group but not in the negative control group. Gait strength and posture were also better maintained in the hWJ-MSC group than in the positive control hADSC group, and were much better than in the negative control group. We observed that when a higher number of hWJ-MSC were added to the transected area, recovery and maintenance of intrinsic muscle function, as evidenced by five-toe spread distances, were also improved. Nerves of better quality were seen in the hWJ-MSC group as demonstrated by fibers with greater numbers of myelinated conducting axons in the distal portion of the regenerated sciatic nerve compared with those of the negative control group. No evidence of local or systemic disruption at the cellular level was seen in the hWJ-MSC group. No aggressive or excessive presence of inflammatory cells in the major organs of the mice was seen after 1 year of operation. A higher level of expression of mRNA for neurotrophic factors NT-3, BDNF, and GDNF was seen in hWJ-MSC compared with hADSC. This group of growth factors has been proven to increase the growth and differentiation of new axons and synapses through a chemoattractant mechanism[43]. They act on the dorsal root ganglions and also promote their survival. The significant increase in expression of these growth factors may be why hWJ-MSC are particularly suited for promotion of peripheral nerve regeneration. In the present study, topically applied hWJ-MSC displayed better nerve regenerative properties than hADSC for transected mouse sciatic nerves.

Although the expression of mRNA for NT-3, BDNF, and GDNF in hWJ-MSC was much higher than in hADSC, the functional recovery of the transected sciatic nerve is only slightly better in the hWJ-MSC group. A possible reason for this, despite a significantly higher level of mRNA neurotrophic factor expression, could be the lack of translation of mRNA to protein levels which actually exert their effect. As such, clinical recovery may not be reflected to the same degree as mRNA levels. Also, the clinical recovery of peripheral nerves may be influenced by a host of other factors and not just the level of neurotrophic factor expression.

Several studies have suggested the possibility of differentiating hWJ-MSC into a neural conduit[44–47] to act as a substitute for nerve gaps but none have examined their direct effects on nerve regeneration in a simple transection model mimicking a situation commonly encountered in clinical practice. Nerve gaps occur when a segment of nerve is missing. Previous reports have described the use of hWJ-MSC seeded in nerve scaffolding made of various materials. The effect of direct addition of hWJ-MSC as used in the present study and the paracrine function of their secretion of neurotrophic growth factors make this a convenient option, in which hWJ-MSC can be directly applied as an adjunct to surgical repair of transected peripheral nerves.

Topical application of various types of multipotent stem cells to transected peripheral nerves has been reported previously. The use of bone marrow stromal cells[48,49], ADSC[50],
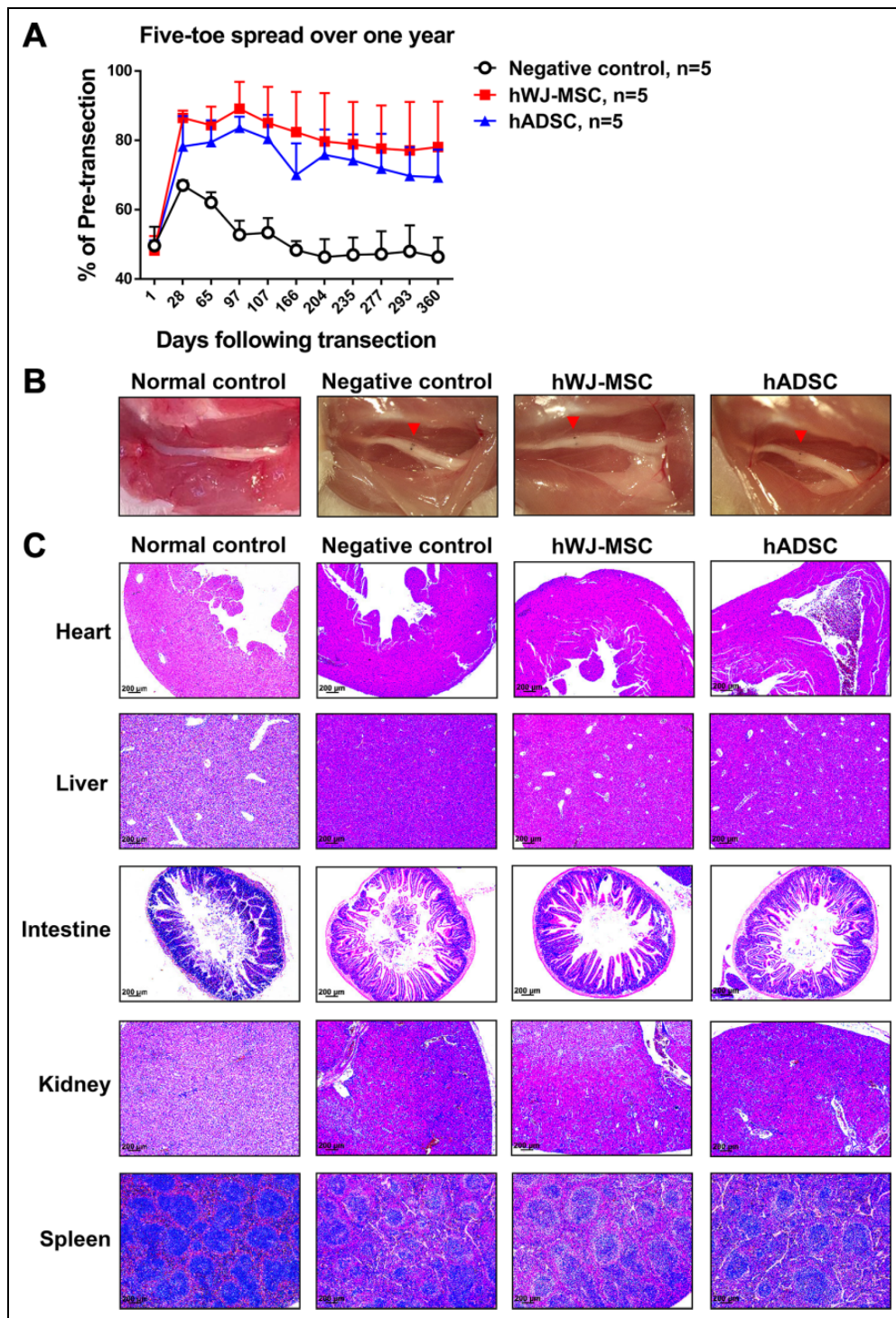
Figure 5. Long-term five-toe spread measurements and safety analysis of hWJ-MSC in mice. (A) Serial measurements of five-toe spread distances in hWJ-MSC, hADSC, and negative control groups after 1 year. The same number of stem cells (5×10^5) was added in both hWJ-MSC and hADSC groups at postoperative day 0. The mean $\pm$ SD of the negative control, hWJ-MSC, and hADSC groups were 62.1 $\pm$ 2.9%, 84.4 $\pm$ 5.3%, and 79.5 $\pm$ 6.3%, respectively, at POD 65. The mean $\pm$ SD of the negative control, hWJ-MSC, and hADSC groups were 46.3 $\pm$ 5.1%, 79.7 $\pm$ 13.9%, and 75.8 $\pm$ 7.3%, respectively, at POD 204. The mean $\pm$ SD of the negative control, hWJ-MSC, and hADSC groups were 46.4 $\pm$ 5.6%, 78.1 $\pm$ 13.1%, and 69.3 $\pm$ 8.1%, respectively, at POD 360. The difference between mean $\pm$ SD of the hWJ-MSC and hADSC groups and negative control was significant (p value < 0.0001, one-way ANOVA; negative control vs. hWJ-MSC, $p < 0.0001$; negative control vs. hADSC, $p < 0.0001$; hWJ-MSC vs. hADSC, $p = 0.0003$; Tukey's test). The average five-toe spread in the normal mouse group was 9.911 $\pm$ 0.04832 mm. (B) Macroscopic appearance of the sciatic nerve and site of cell therapy after 1 year in normal control, negative control, hWJ-MSC, and hADSC groups. The red arrow represents the site of surgical repair. Normal control group represents the normal appearance of the sciatic nerve without nerve anastomotic repair and cell administration. (C) Hematoxylin and eosin staining of various organs from all four groups, demonstrating regular architecture and no abnormal growths. The data were collected from five mice in each group.
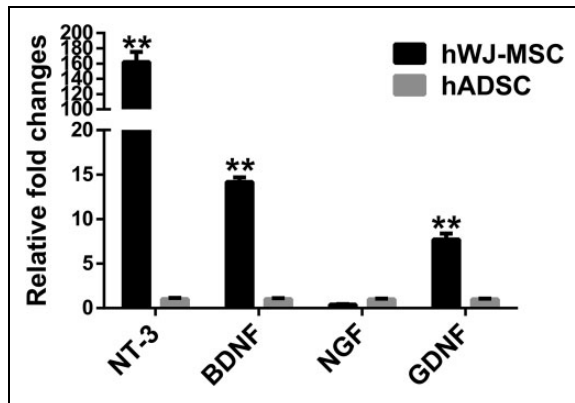
Figure 6. Quantification of hWJ-MSC-derived neurotrophic factor expression. The expression of mRNA for neurotrophic factors such as neurotrophic factor 3 (NT-3), brain-derived neurotrophic factor (BDNF), neurotrophic growth factor (NGF), and glial-derived neurotrophic factor (GDNF) in hWJ-MSC and hADSC was quantified using qPCR. The neurotrophic factor expression was normalized to that of GAPDH. The relative fold changes (mean $\pm$ SD) of hWJ-MSC and hADSC groups were 161.9 $\pm$ 13.3 and 1.0 $\pm$ 0.1, respectively, for NT-3 expression. The relative fold changes (mean $\pm$ SD) of hWJ-MSC and hADSC groups were 14.2 $\pm$ 0.5 and 1.0 $\pm$ 0.1, respectively, for BDNF expression. The relative fold changes (mean $\pm$ SD) of hWJ-MSC and hADSC groups were 0.4 $\pm$ 0.1 and 1.0 $\pm$ 0.1, respectively, for NGF expression. The relative fold changes (mean $\pm$ SD) of hWJ-MSC and hADSC groups were 7.7 $\pm$ 0.7 and 1.0 $\pm$ 0.1, respectively, for GDNF expression. The difference between mean $\pm$ SD of the hWJ-MSC and hADSC groups was significant ($p < 0.005$, Student's t-test).

and neural crest cells differentiated from stem cell precursors has been reported as a topical form of cell therapy in peripheral nerve regeneration. However, variable degrees of success have been reported in animal models, and the various sources of cells may not be easily obtained. hWJ-MSC are easily obtained from the umbilical cord of fetuses and can be banked[51].

The levels of immunogenicity are also crucial in ensuring the survival of cells and the establishment of a cell bank for cell therapy. hWJ-MSC have been shown to be negative for major histocompatibility complex class (MHC) II and possess a low expression of MHC class I[24,25]. Harvesting a patient's own cells and processing them for autologous transfer can be tedious and increases the cost of therapy. Because hWJ-MSC have low immunogenicity, they may be transferred from one person to another; therefore, a cell bank can be established and applied when required. This may be a more direct method of clinical application, and suggest that hWJ-MSC are feasible for use as an allogeneic cell bank that can be used readily for cell therapy.

hWJ-MSC have also been shown to be able to differentiate to Schwann-like cells that can contribute to peripheral nerve regeneration[46]. The secretion of neurotrophic factors such as BDNF, NGF, and NT-3 can accelerate and trigger axonal regrowth, which may contribute to accelerated nerve

repair. The low immunogenicity of hWJ-MSC makes them a potentially clinically applicable form of cell therapy for enhancing nerve regeneration. hWJ-MSC are derived from fetal umbilical cords that are normally discarded and that contain a high number of multipotent stem cells. Their availability and the potency of such multipotent stem cells make umbilical cords a convenient source for a cell bank. Indeed, in this study examining the effects of hWJ-MSC on transected peripheral nerve regeneration in mice, we showed that as few as 5×10^5 hWJ-MSC are required for nerve regeneration, which makes them relatively more potent than other types of MSC. Thus, hWJ-MSC not only exert immunomodulatory effects to allow allograft survival[52,53], they also accelerate peripheral nerve recovery and regeneration. Topical administration of hWJ-MSC bound to a delivery agent such as hydrogel may even provide sustained therapeutic effects with localized delivery of cells to the affected area. In vascularized composite allotransplantation, which is the current method for replacing limbs or faces like-for-like, two challenges remain, namely allograft rejection and nerve regeneration. For example, for a transplanted limb to be useful, its functional recovery must be ensured in addition to overcoming the rejection issue. Thus, recovery of the peripheral nerves is key to improving the function of transplanted limbs, and local delivery of hWJ-MSC therapies may provide hope for promoting peripheral nerve regeneration in the allotransplanted functional limb.

Acknowledgments

Ethical Approval

The study protocol was approved by the Ethics Committee of the Institutional Animal Care and Use Committee Chang Gung Memorial Hospital, Taiwan (No. 2016011903, No. 2016031109, No. 2017121001 and No. 2018080701 for animals).

Statement of Human and Animal Rights

All animal procedures were performed according to protocols approved by the Institutional Animal Care and Use Committee in Chang Gung Memorial Hospital. Human subjects were not used in this study.

Statement of Informed Consent

There are no human subjects in this article and informed consent is not applicable.

Declaration of Conflicting Interests

The author(s) declared no potential conflicts of interest with respect to the research, authorship, and/or publication of this article.

ORCID iD

Aline Yen Ling Wang https://orcid.org/0000-0001-6272-6948

Supplemental Material

Supplemental material for this article is available online.

References

1. Gordon T. Nerve regeneration: understanding biology and its influence on return of function after nerve transfers. Hand Clin. 2016;32(2):103–117.

2. Li GY, Xue MQ, Wang JW, Zeng XY, Qin J, Sha K. Traumatic brachial plexus injury: a study of 510 surgical cases from multicenter services in Guangxi, China. Acta Neurochir (Wien). 2019. [Epub ahead of print].

3. Li R, Liu Z, Pan Y, Chen L, Zhang Z, Lu L. Peripheral nerve injuries treatment: a systematic review. Cell Biochem Biophys. 2014;68(3):449–454.

4. Pederson WC. Median nerve injury and repair. J Hand Surg Am. 2014;39(6):1216–1222.

5. He B, Zhu Z, Zhu Q, Zhou X, Zheng C, Li P, Zhu S, Liu X, Zhu J. Factors predicting sensory and motor recovery after the repair of upper limb peripheral nerve injuries. Neural Regen Res. 2014;9(6):661–672.

6. Novak CB, Anastakis DJ, Beaton DE, Katz J. Patient-reported outcome after peripheral nerve injury. J Hand Surg Am. 2009; 34(2):281–287.

7. Lao WW, Wang YL, Ramirez AE, Cheng HY, Wei FC. A new rat model for orthotopic abdominal wall allotransplantation. Plast Reconstr Surg Glob Open. 2014;2(4):e136.

8. Loh CYY, Wang AYL, Tiong VTY, Athanassopoulos T, Loh M, Lim P, Kao HK. Animal models in plastic and reconstructive surgery simulation-a review. J Surg Res. 2018;221: 232–245.

9. Wang AYL, Loh CYY. Reviewing immunosuppressive regimens in animal models for vascularized composite allotransplantation. Plast Aesthet Res. 2018;5:10.

10. Wei FC, Ma HS, Chien YY, Dellon AL. Effect of neurotization upon degree of sensory recovery in toe-to-hand microvascular transplantation. J Reconstr Microsurg. 2012;28(6):367–370.

11. Kern B, Budihardjo JD, Mermulla S, Quan A, Cadmi C, Lopez J, Khusheim M, Xiang S, Park J, Furtmüller GJ, Sarhane KA, et al. A novel rodent orthotopic forelimb transplantation model that allows for reliable assessment of functional recovery resulting from nerve regeneration. Am J Transplant. 2017; 17(3):622–634.

12. Marques M, Correia-Sá I, Festas MJ, Silva S, Silva AI, Silva A, Amarante J. Six years of follow-up after bilateral hand replantation. Chir Main. 2013;32(4):226–234.

13. Rinker B, Zoldos J, Weber RV, Ko J, Thayer W, Greenberg J, Leversedge FJ, Safa B, Buncke G. Use of processed nerve allografts to repair nerve injuries greater than 25 mm in the hand. Ann Plast Surg. 2017;78(6S suppl 5): S292–S295.

14. Shores JT, Imbriglia JE, Lee WP. The current state of hand transplantation. J Hand Surg Am. 2011;36(11):1862–1867.

15. Akdeniz ZD, Bayramiçli M, Ateş F, Özkan N, Yucesoy CA, Ercan F. The role of botulinum toxin type a-induced motor endplates after peripheral nerve repair. Muscle Nerve. 2015; 52(3):412–418.

16. Sakakima H, Yoshida Y, Yamazaki Y, Matsuda F, Ikutomo M, Ijiri K, Muramatsu H, Muramatsu T, Kadomatsu K. Disruption of the midkine gene (Mdk) delays degeneration and regeneration in injured peripheral nerve. J Neurosci Res. 2009;87(13): 2908–2915.

17. Wang J, Sun J, Tang Y, Guo G, Zhou X, Chen Y, Shen M. Basic fibroblast growth factor attenuates the degeneration of injured spinal cord motor endplates. Neural Regen Res. 2013; 8(24):2213–2224.

18. Chung T, Park JS, Kim S, Montes N, Walston J, Höke A. Evidence for dying-back axonal degeneration in age-associated skeletal muscle decline. Muscle Nerve. 2017; 55(6):894–901.

19. Dixon RW, Harris JB. Nerve terminal damage by beta-bungarotoxin: its clinical significance. Am J Pathol. 1999; 154(2):447–455.

20. Richardson SM, Kalamegam G, Pushparaj PN, Matta C, Memic A, Khademhosseini A, Mobasheri R, Poletti FL, Hoyland JA, Mobasheri A. Mesenchymal stem cells in regenerative medicine: focus on articular cartilage and intervertebral disc regeneration. Methods. 2016;99:69–80.

21. Can A, Celikkan FT, Cinar O. Umbilical cord mesenchymal stromal cell transplantations: a systemic analysis of clinical trials. Cytotherapy. 2017;19(12):1351–1382.

22. Joerger-Messerli MS, Marx C, Oppliger B, Mueller M, Surbek DV, Schoeberlein A. Mesenchymal stem cells from Wharton's jelly and amniotic fluid. Best Pract Res Clin Obstet Gynaecol. 2016;31:30–44.

23. Wang HS, Hung SC, Peng ST, Huang CC, Wei HM, Guo YJ, Fu YS, Lai MC, Chen CC. Mesenchymal stem cells in the Wharton's jelly of the human umbilical cord. Stem Cells. 2004;22(7):1330–1337.

24. Weiss ML, Anderson C, Medicetty S, Seshareddy KB, Weiss RJ, VanderWerff I, Troyer D, McIntosh KR. Immune properties of human umbilical cord Wharton's jelly-derived cells. Stem Cells. 2008;26(11):2865–2874.

25. Nagamura-Inoue T, He H. Umbilical cord-derived mesenchymal stem cells: their advantages and potential clinical utility. World J Stem Cells. 2014;6(2):195–202.

26. Kingham PJ, Kolar MK, Novikova LN, Novikov LN, Wiberg M. Stimulating the neurotrophic and angiogenic properties of

human adipose-derived stem cells enhances nerve repair. Stem Cells Dev. 2014;23(7):741–754.

27. Abbas OL, Borman H, Uysal ÇA, Gönen ZB, Aydin L, Helvacıoğlu F, Ilhan Ş, Yazici AC. Adipose-derived stem cells enhance axonal regeneration through cross-facial nerve grafting in a rat model of facial paralysis. Plast Reconstr Surg. 2016; 138(2):387–396.

28. Sowa Y, Kishida T, Imura T, Numajiri T, Nishino K, Tabata Y, Mazda O. Adipose-derived stem cells promote peripheral nerve regeneration in vivo without differentiation into Schwann-like lineage. Plast Reconstr Surg. 2016;137(2): 318e–330e.

29. di Summa PG, Kingham PJ, Raffoul W, Wiberg M, Terenghi G, Kalbermatten DF. Adipose-derived stem cells enhance peripheral nerve regeneration. J Plast Reconstr Aesthet Surg. 2010;63(9):1544–1552.

30. Loh CY, Wang AY, Kao HK, Cardona E, Chuang SH, Wei FC. Episomal induced pluripotent stem cells promote functional recovery of transected murine peripheral nerve. Plos One. 2016;11(10):e0164696.

31. IJkema-Paassen J, Jansen K, Gramsbergen A, Meek MF. Transection of peripheral nerves, bridging strategies and effect evaluation. Biomaterials. 2004;25(9):1583–1592.

32. Griffin JW, Pan B, Polley MA, Hoffman PN, Farah MH. Measuring nerve regeneration in the mouse. Exp Neurol. 2010; 223(1):60–71.

33. Garcia ML, Rao MV, Fujimoto J, Garcia VB, Shah SB, Crum J, Gotow T, Uchiyama Y, Ellisman M, Calcutt NA, Cleveland DW. Phosphorylation of highly conserved neurofilament medium KSP repeats is not required for myelin-dependent radial axonal growth. J Neurosci. 2009;29(5): 1277–1284.

34. Lee JY, Giusti G, Wang H, Friedrich PF, Bishop AT, Shin AY. Functional evaluation in the rat sciatic nerve defect model: a comparison of the sciatic functional index, ankle angles, and isometric tetanic force. Plast Reconstr Surg. 2013;132(5): 1173–1180.

35. Canan S, Bozkurt HH, Acar M, Vlamings R, Aktas A, Sahin B, Temel Y, Kaplan S. An efficient stereological sampling approach for quantitative assessment of nerve regeneration. Neuropathol Appl Neurobiol. 2008;34(6):638–649.

36. Jortner BS. Preparation and analysis of the peripheral nervous system. Toxicol Pathol. 2011;39(1):66–72.

37. Ge J, Zhu S, Yang Y, Liu Z, Hu X, Huang L, Quan X, Wang M, Huang J, Li Y, Luo Z. Experimental immunological demyelination enhances regeneration in autograft-repaired long peripheral nerve gaps. Sci Rep. 2016;6:39828.

38. Triolo D, Dina G, Taveggia C, Vaccari I, Porrello E, Rivellini C, Domi T, La Marca R, Cerri F, Bolino A, Quattrini A, et al. Vimentin regulates peripheral nerve myelination. Development. 2012;139(7):1359–1367.

39. Chomiak T, Hu B. What is the optimal value of the g-ratio for myelinated fibers in the rat CNS? A theoretical approach. Plos One. 2009;4(11):e7754.

40. Benninger Y, Colognato H, Thurnherr T, Franklin RJ, Leone DP, Atanasoski S, Nave KA, Ffrench-Constant C,

Suter U, Relvas JB. Beta1-integrin signaling mediates premyelinating oligodendrocyte survival but is not required for CNS myelination and remyelination. J Neurosci. 2006; 26(29):7665–7673.

41. Duval T, Le Vy S, Stikov N, Campbell J, Mezer A, Witzel T, Keil B, Smith V, Wald LL, Klawiter E, Cohen-Adad J. g-Ratio weighted imaging of the human spinal cord in vivo. Neuroimage. 2017;145(Pt A):11–23.

42. Campbell JSW, Leppert IR, Narayanan S, Boudreau M, Duval T, Cohen-Adad J, Pike GB, Stikov N. Promise and pitfalls of g-ratio estimation with MRI. Neuroimage. 2018; 182:80–96.

43. Zhu G, Sun C, Liu W. Effects of neurotrophin-3 on the differentiation of neural stem cells into neurons and oligodendrocytes. Neural Regen Res. 2012;7(19):1483–1487.

44. Shalaby SM, El-Shal AS, Ahmed FE, Shaban SF, Wahdan RA, Kandel WA, Senger MS. Combined Wharton's jelly derived mesenchymal stem cells and nerve guidance conduit: a potential promising therapy for peripheral nerve injuries. Int J Biochem Cell Biol. 2017;86:67–76.

45. Jadalannagari S, Aljitawi OS. Ectodermal differentiation of Wharton's jelly mesenchymal stem cells for tissue engineering and regenerative medicine applications. Tissue Eng Part B Rev. 2015;21(3):314–322.

46. Peng J, Wang Y, Zhang L, Zhao B, Zhao Z, Chen J, Guo Q, Liu S, Sui X, Xu W, Lu S. Human umbilical cord Wharton's jelly-derived mesenchymal stem cells differentiate into a Schwann-cell phenotype and promote neurite outgrowth in vitro. Brain Res Bull. 2011;84(3):235–243.

47. Gärtner A, Pereira T, Alves MG, Armada-da-Silva PA, Amorim I, Gomes R, Ribeiro J, França ML, Lopes C, Carvalho RA, Socorro S, et al. Use of poly(DL-lactide-epsilon-caprolactone) membranes and mesenchymal stem cells from the Wharton's jelly of the umbilical cord for promoting nerve regeneration in axonotmesis: in vitro and in vivo analysis. Differentiation. 2012;84(5):355–365.

48. Chen CJ, Ou YC, Liao SL, Chen WY, Chen SY, Wu CW, Wang CC, Wang WY, Huang YS, Hsu SH. Transplantation of bone marrow stromal cells for peripheral nerve repair. Exp Neurol. 2007;204(1):443–453.

49. Dezawa M, Takahashi I, Esaki M, Takano M, Sawada H. Sciatic nerve regeneration in rats induced by transplantation of in vitro differentiated bone-marrow stromal cells. Eur J Neurosci. 2001;14(11):1771–1776.

50. Allbright KO, Bliley JM, Havis E, Kim DY, Dibernardo GA, Grybowski D, Waldner M, James IB, Sivak WN, Rubin JP, Marra KG. Delivery of adipose-derived stem cells in poloxamer hydrogel improves peripheral nerve regeneration. Muscle Nerve. 2018;58(2):251–260.

51. Chatzistamatiou TK, Papassavas AC, Michalopoulos E, Gamaloutsos C, Mallis P, Gontika I, Panagouli E, Koussoulakos SL, Stavropoulos-Giokas C. Optimizing isolation culture and freezing methods to preserve Wharton's jelly's mesenchymal stem cell (MSC) properties: an MSC banking protocol validation for the Hellenic Cord Blood Bank. Transfusion. 2014; 54(12):3108–3120.

52. Qiu Y, Yun MM, Han X, Zhao R, Zhou E, Yun S. Human umbilical cord mesenchymal stromal cells suppress MHC class II expression on rat vascular endothelium and prolong survival time of cardiac allograft. Int J Clin Exp Med. 2014;7(7): 1760–1767.

53. Donders R, Vanheusden M, Bogie JF, Ravanidis S, Thewissen K, Stinissen P, Gyselaers W, Hendriks JJ, Hellings N. Human Wharton's jelly-derived stem cells display immunomodulatory properties and transiently improve rat experimental autoimmune encephalomyelitis. Cell Transplant. 2015;24(10):2077–2098.